Universität Stuttgart

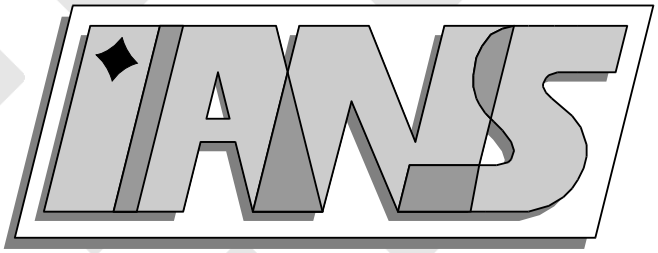

A fast and robust method for contact problems by combining a primal-dual active set strategy and algebraic multigrid methods

S.Brunssen, F.Schmid, M.Schäfer, B.Wohlmuth

Berichte aus dem Institut für Angewandte Analysis und Numerische Simulation

Preprint 2005/010

Universität Stuttgart

A fast and robust method for contact problems by combining a primal-dual active set strategy and algebraic multigrid methods

S.Brunssen, F.Schmid, M.Schäfer, B.Wohlmuth

Berichte aus dem Institut für Angewandte Analysis und Numerische Simulation

Preprint 2005/010

Institut für Angewandte Analysis und Numerische Simulation (IANS)
Fakultät Mathematik und Physik
Fachbereich Mathematik
Pfaffenwaldring 57
D-70 569 Stuttgart

E-Mail: ians-preprints@mathematik.uni-stuttgart.de
WWW: http://preprints.ians.uni-stuttgart.de

ISSN **1611-4176**

A fast and robust method for contact problems by combining a primal-dual active set strategy and algebraic multigrid methods

S. BRUNSSEN, F. SCHMID, M. SCHAEFER AND B. WOHLMUTH

Abstract

In order to extend the usability of implicit FE codes for large scale forming simulations, the computation time has to be decreased dramatically. This can in principle be achieved by using iterative solvers. However, due to the presence of contact, the stiffness matrices turn out to be severly ill-conditioned. The work detailed in this paper shows that a contact algorithm based on a primal-dual active set strategy provides significant advantages over a penalty formulation. It does not deteriorate the condition number and is therefore highly efficient with respect to computation time in combination with fast iterative solvers especially algebraic multigrid methods.

1 Introduction

The efficient treatment of contact problems is crucial to the performance of FE codes in the context of metal forming. Efficient contact algorithms have been developed in recent years, see [15, 16, 21, 22, 23, 24] and the references therein. In contrast to the commonly used penalty method, the primal-dual active-set strategy, which is in the following referred to as active-set strategy [12], allows one to adjust the geometric constraints of the tool exactly in a weak integral sense. Thus, the deterioration of the condition number of the stiffness matrix which arises in penalty formulations can be avoided by that method. We will see that this strategy is very attractive for use in metal forming, especially in combination with iterative solvers, as their convergence behavior strongly depends on the condition number of the system matrix. Due to steady increase in problem size and the need for a robust, highly accurate and scalable solution method, algebraic multigrid methods are the main focus of this investigation [6, 19].
In the present paper, we adapt the active set strategy for nonlinear material-behavior and give some details about the implementation in LARSTRAN/SHAPE [8], a FE-package dedicated to large-strain plasticity in the context of metal forming simulations. Furthermore it will be shown, that in combination with the active set strategy, the well known good complexity of multigrid methods can be achieved. By the use of algebraic multigrid, problem dependency can be overcome such that the used solver provides a black-box character. In addition we show that a so-called Newton-inexact respectively AMG-inexact strategy can be employed. This means in the first case that the two nonlinearities of material behavior and contact can be handled in only one Newton loop. In the latter case, it is shown that the Newton and the solver loop of the algebraic multigrid method can be merged similarly. Both strategies provide further decrease in computation time.
The paper is organized as follows. In Section 2, the active set strategy is explained in theory. Section 3 deals with the implementation of the method with special emphasis on the iterative solution procedure including the description of the algebraic multigrid method used. In Section 4, we introduce a nonlinear 3D frictionless contact problem which is solved with a Newton-Raphson method and different direct and iterative solvers. Numerical examples on the inexact strategies will be given and a comparison in the behavior of the algebraic multigrid method in combination with the active set strategy and a penalty approach is discussed. Finally we give an elasto-plastic example to show that the proposed method is independent of the material model.

2 Active set strategy

To handle the nonlinearity of the (Karush–Kuhn–Tucker) contact conditions, we apply a primal-dual active set strategy based on dual Lagrange multipliers [12, 13, 20], which can be interpreted as a Newton method [12], and adapt it for nonlinear material-behavior. In contrast to the commonly used penalty method [14], the active-set strategy allows to adjust the geometric constraints of the tool exactly in a weak integral sense. The contact stress can be easily recovered from the displacements in a variational consistent way and does not depend on a tuning parameter.

2.1 Basic idea

As an example of a forming operation, we consider a rectangular workpiece which is indented by a rigid, hemispherical punch, see Figure 1a. We denote by $\mathcal{S}$ the set of potential contact nodes, see Figure 1a. Let us consider the loadstep, when the tool comes in contact with the workpiece for the first time. Let k be the iteration index for the active set loop. Let $\mathcal{A}_k \subset \mathcal{S}$ be the active set, for which the body is in contact with the obstacle. The complementary set $\mathcal{I}_k := \mathcal{S} - \mathcal{A}_k$ is called the inactive set for all steps $k = 1, \ldots$ until convergence of the active set. Let us consider the following simple test example to understand how the sets $\mathcal{I}_{k+1}$ and $\mathcal{A}_{k+1}$ are correctly determined. Let us assume in the k-th step the following situation, see Figure 1b:

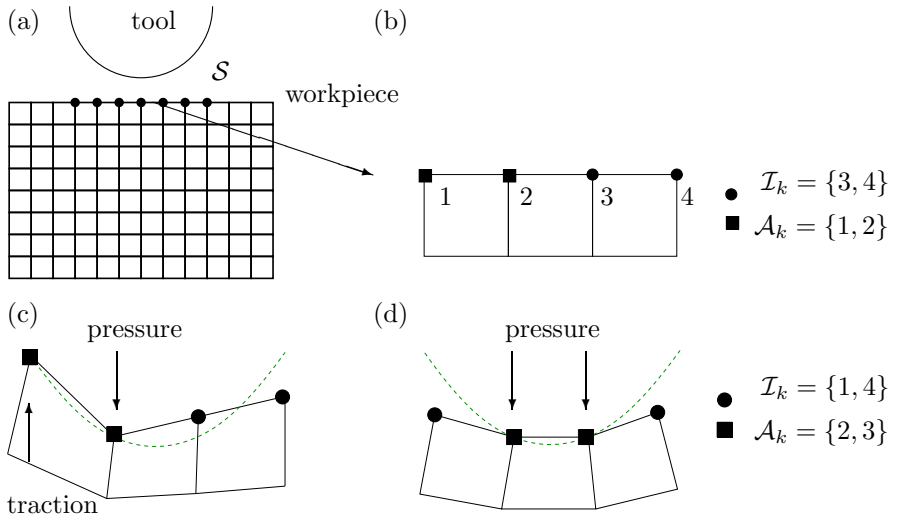

Figure 1: Active set strategy

Nodes {1,2} are active, nodes {3,4} are inactive. The tool geometry is then adjusted to the active nodes, no matter if the active set is already correct or not, see Figure 1c. Now the nodal forces and the detected penetration are used to update the active and inactive node sets:

$$\begin{aligned} \mathcal{A}_{k+1} &= \{p \in \mathcal{I}_k : p \text{ penetrates}\} \cup \{p \in \mathcal{A}_k : p \text{ under compression}\} \\ \mathcal{I}_{k+1} &= \{p \in \mathcal{I}_k : \text{no penetration}\} \cup \{p \in \mathcal{A}_k : p \text{ under tension}\}. \end{aligned}$$

Then the restrictions from the tool geometry are again adjusted to the correct active nodes and the inactive nodes are released, see Figure 1d. The step from (c) to (d) is one step of the active set iteration which can be run parallel to the Newton iteration for the nonlinear material law. This is possible because the search for the correct active set can also be interpreted as a Newton iteration. More details will be given in Section 3.

2.2 Theory and algorithm

Algorithm 1 Primal-dual active set algorithm

1: **Initialize** $\mathcal{A}_1$ and $\mathcal{I}_1$, such that $\mathcal{S} = \mathcal{A}_1 \cup \mathcal{I}_1$ and $\mathcal{A}_1 \cap \mathcal{I}_1 = \emptyset$ and set $k = 1$.
2: **Find** the primal-dual pair $(\boldsymbol{u}^k, \boldsymbol{\lambda}^k)$:
3: $\quad \boldsymbol{F}(\boldsymbol{u}^k) + \mathbf{B}\boldsymbol{\lambda}^k = 0$,
4: $\quad u^k_{n,p} = g_p \quad$ for all $\quad p \in \mathcal{A}_k$,
5: $\quad \lambda^k_{n,p} = 0 \quad$ for all $\quad p \in \mathcal{I}_k$,
6: $\quad \boldsymbol{\lambda}^k_{T,p} = \mathbf{0} \quad$ for all $\quad p \in \mathcal{S}$.
7: **Set** $\mathcal{A}_{k+1}$ and $\mathcal{I}_{k+1}$ to
8: $\quad \mathcal{A}_{k+1} := \left\{p \in \mathcal{S} \,:\, \lambda^k_{n,p} + c(u^k_{n,p} - g_p) > 0\right\}$,
9: $\quad \mathcal{I}_{k+1} := \left\{p \in \mathcal{S} \,:\, \lambda^k_{n,p} + c(u^k_{n,p} - g_p) \leq 0\right\}$.
10: **if** $\mathcal{A}_{k+1} = \mathcal{A}_k$ **and** $\mathcal{I}_{k+1} = \mathcal{I}_k$, **then**
11: $\quad$ stop
12: **else**
13: $\quad$ set $k = k + 1$ and **goto** step (2).
14: **end if**

For a linear material law the primal-dual active set strategy is explained in [13]. We will show that the method is also applicable for geometric nonlinear and nonlinear material behavior. We denote by $\mathbf{V}$ the space of test functions fulfilling $\boldsymbol{v} = 0$ on the Dirichlet boundary Γ_D and by $\mathbf{V}_h \subset \mathbf{V}$ the approximating finite element space. Let $\boldsymbol{u} \in \mathbf{V}$ be the displacements and let $\boldsymbol{\sigma}(\boldsymbol{u})$ be Cauchy's stress tensor depending nonlinearly on $\boldsymbol{u}$ for example according to an elasto-plastic material law.

Continuous equations It is assumed that a workpiece $\Omega \subset \mathbb{R}^d, d \in \{2, 3\}$, comes into contact with a rigid tool with the boundary $\Gamma_{\mathbf{tool}}$. We introduce the following notations: The part of $\partial\Omega$ which comes in contact with $\Gamma_{\mathbf{tool}}$ is called $\Gamma_C \subset \mathbb{R}^{d-1}$. Let us denote with $\boldsymbol{x}_{\mathbf{ref}} \in \Gamma_C$ the coordinates of an arbitrary point in the reference configuration on the potential contact zone. In the actual configuration it has the coordinates $\boldsymbol{x}_{\mathbf{act}}(\boldsymbol{x}_{\mathbf{ref}})$. To avoid difficulties arising from large deformations the reference configuration must be chosen in such a way that the deformation from the reference configuration to the actual configuration is small. Like in Updated Lagrange, it is a good choice to take the last time step as reference configuration. We call $\boldsymbol{x}_{\mathbf{tool}}(\boldsymbol{x}_{\mathbf{ref}})$ the corresponding point on the tool boundary $\Gamma_{\mathbf{tool}}$. If we can describe $\Gamma_{\mathbf{tool}}$ by a sufficiently smooth function, we can define on every point on $\Gamma_{\mathbf{tool}}$ the outward normal $\boldsymbol{n}$ on the tool such that the following closest point relation holds:

$$\begin{aligned} ||\boldsymbol{x}_{\mathbf{tool}}(\boldsymbol{x}_{\mathbf{ref}}) - \boldsymbol{x}_{\mathbf{ref}}||_2 &\rightarrow min \\ \boldsymbol{x}_{\mathbf{tool}}(\boldsymbol{x}_{\mathbf{ref}}) - \boldsymbol{x}_{\mathbf{ref}} &= -g(\boldsymbol{x}_{\mathbf{ref}})\boldsymbol{n}(\boldsymbol{x}_{\mathbf{ref}}), \end{aligned} \tag{1}$$

where $g(\boldsymbol{x}_{\mathbf{ref}})$ denotes the gap between $\boldsymbol{x}_{\mathbf{tool}}(\boldsymbol{x}_{\mathbf{ref}})$ and $\boldsymbol{x}_{\mathbf{ref}}$. So the gap has the meaning of the distance between the tool and the structure in the reference configuration. By $\boldsymbol{u}(\boldsymbol{x}_{\mathbf{ref}}) := \boldsymbol{x}_{\mathbf{ref}} - \boldsymbol{x}_{\mathbf{act}}$ we denote the displacements. In the following we will always write $\boldsymbol{u}$ instead of $\boldsymbol{u}(\boldsymbol{x}_{\mathbf{ref}})$, $\boldsymbol{n}$ instead of $\boldsymbol{n}(\boldsymbol{x}_{\mathbf{ref}})$ and g instead of $g(\boldsymbol{x}_{\mathbf{ref}})$ and we will assume that the relation (1) holds. Finally we define the scalar valued normal part $\sigma_n(\boldsymbol{u})$ of the stresses on Γ_C and the tangential stress vector $\boldsymbol{\sigma}_T(\boldsymbol{u}) \in \mathbb{R}^d$ by

$$\sigma_n(\boldsymbol{u}) := (\boldsymbol{\sigma}(\boldsymbol{u})\,\boldsymbol{n})\,\boldsymbol{n}, \qquad \boldsymbol{\sigma}_T(\boldsymbol{u}) := \boldsymbol{\sigma}(\boldsymbol{u})\,\boldsymbol{n} - \sigma_n(\boldsymbol{u})\,\boldsymbol{n}. \tag{2}$$

The contact conditions for all $\boldsymbol{x}_{\mathbf{ref}}$ in the potential contact zone Γ_C are given by

$$\begin{aligned} \boldsymbol{u} \cdot \boldsymbol{n} - g &\leq 0, && (3)\\ \sigma_n(\boldsymbol{u}) &\leq 0, && (4)\\ \sigma_n(\boldsymbol{u})\,(\boldsymbol{u} \cdot \boldsymbol{n} - g) &= 0, && (5)\\ \boldsymbol{\sigma}_T\,(\boldsymbol{u}) &= 0. && (6) \end{aligned}$$

(3) means that no penetration is allowed and

(4) means there is only compression allowed and no tension, since there is no adhesion

(5) is the complementary condition that means that either non-zero contact stresses are present and the gap is zero or the gap is non-zero and and there are no contact stresses. Finally

(6) means the stress in tangential direction is zero, because we have no friction.

The equilibrium is given by (for simplicity we assume volume forces and other external forces to be zero except from the contact forces): Find $\boldsymbol{u} \in \mathbf{V}$ such that:

$$\boldsymbol{F}(\boldsymbol{u}, \delta\boldsymbol{v}) + \int_{\Gamma_C} \boldsymbol{\lambda} \cdot \delta\boldsymbol{v}\; ds \stackrel{!}{=} 0 \tag{7}$$

for an arbitrary test function $\delta\boldsymbol{v} \in \mathbf{V}$ and with internal forces $\boldsymbol{F}$ depending nonlinearly on $\boldsymbol{u}$.

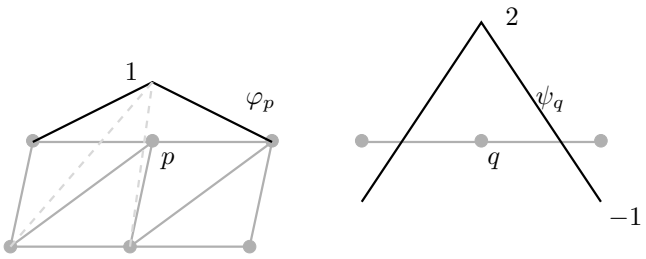

Figure 2: Shape functions

The Lagrange multipliers $\boldsymbol{\lambda} := -\boldsymbol{\sigma}(\boldsymbol{u})\boldsymbol{n}$ are exactly the contact forces which are necessary to adjust the contact-displacements on the contact boundary Γ_C. These are introduced as additional unknowns to fulfill the contact conditions.

Discretized form The displacements $\boldsymbol{u}$ are approximated by the space $\mathbf{V}_h = \text{span}\{\varphi_p\}^d$ and the Lagrange multipliers $\boldsymbol{\lambda}$ are approximated by $\mathbf{M}_h = \text{span}\{\psi_q\}^d$ with the 1-dimensional basis-functions, φ_p and ψ_q which are associated with the node p resp. node q, see Figure 2 in the special case of 2D linear trial functions. For simplicity of notation, we use the same symbol for a function in $\mathbf{V}_h$ and $\mathbf{M}_h$ as for its algebraic representation with respect to the nodal basis. Let $\boldsymbol{u} \in \mathbf{V}_h$ and $\boldsymbol{\lambda} \in \mathbf{M}_h$ be the solution of the FE-discretization of the equilibrium (7). For the discretization of the space $\mathbf{M}_h$, we use dual Lagrange multipliers, see [20]. We refer to [2, 3] and the references therein for an overview of the mortar method for nonlinear contact problems.
Then the algebraic representation of (7) has the form

$$\boldsymbol{F}(\boldsymbol{u}) + \mathbf{B}\boldsymbol{\lambda} = 0, \tag{8}$$

with

$$\mathbf{B}[p,q] := \int_{\Gamma_C} \varphi_p \psi_q \, ds\; \mathbf{I}_d, \qquad p = 1, \ldots, n_{\mathbf{nodes}}, q = 1, \ldots, n_{\mathbf{contactnodes}},$$

where $\mathbf{I}_d$ denotes the identity matrix in $\mathbb{R}^{d\times d}$. The biorthogonality of the basis functions yields

$$\int_{\Gamma_C} \varphi_p \psi_q \, ds = \theta_{pq} \int_{\Gamma_C} \varphi_p \, ds, \tag{9}$$

with

$$\theta_{pq} = \begin{cases} 1 & \text{structure node } p \text{ coincides with potential contact node } q, \\ 0 & \text{otherwise.} \end{cases}$$

To examine the structure of $\mathbf{B}$, we introduce two sets of indices $\mathcal{S}$ and $\mathcal{N}$. The elements of $\mathcal{S}$ are the vertices on Γ_C, in other words the potential contact nodes, and $\mathcal{N}$ contains all other vertices. Now, using an appropriate node numbering, $\mathbf{B}$ has the form $\mathbf{B} = (\mathbf{0}\ \mathbf{D})^\top$, where due to (9) the entries of the diagonal matrix $\mathbf{D}$ are given by

$$\mathbf{D}[p,q] = \theta_{pq} \mathbf{I}_d \cdot \int_{\Gamma_C} \varphi_p \, ds. \tag{10}$$

We can write the Newton step for $i-1$ to i of (8) as

$$\mathbf{A}\boldsymbol{u}^i + \mathbf{B}\boldsymbol{\lambda} = \mathbf{A}\boldsymbol{u}^{i-1} - \boldsymbol{F}(\boldsymbol{u}^i)$$

or algebraically

$$\begin{bmatrix} \mathbf{A}_{\mathcal{N}\mathcal{N}} & \mathbf{A}_{\mathcal{N}\mathcal{S}} & \mathbf{0} \\ \mathbf{A}_{\mathcal{S}\mathcal{N}} & \mathbf{A}_{\mathcal{S}\mathcal{S}} & \mathbf{D} \end{bmatrix} \begin{bmatrix} \boldsymbol{u}^i_{\mathcal{N}} \\ \boldsymbol{u}^i_{\mathcal{S}} \\ \boldsymbol{\lambda}_{\mathcal{S}} \end{bmatrix} = \begin{bmatrix} \mathbf{A}_{\mathcal{N}\mathcal{N}} & \mathbf{A}_{\mathcal{N}\mathcal{S}} \\ \mathbf{A}_{\mathcal{S}\mathcal{N}} & \mathbf{A}_{\mathcal{S}\mathcal{S}} \end{bmatrix} \begin{bmatrix} \boldsymbol{u}^{i-1}_{\mathcal{N}} \\ \boldsymbol{u}^{i-1}_{\mathcal{S}} \end{bmatrix} - \begin{bmatrix} \boldsymbol{F}_{\mathcal{N}}(u^i) \\ \boldsymbol{F}_{\mathcal{S}}(\boldsymbol{u}^i) \end{bmatrix},$$

with $\mathbf{A} := \partial \boldsymbol{F}(\boldsymbol{u}^i)$ the Jacobian of $\boldsymbol{F}$ and $\boldsymbol{u}^i$ is the displacement in the ith Newton step and in the kth active set iteration step, where k is fixed. The index i is omitted at $\boldsymbol{\lambda}$ because only the displacements $\boldsymbol{u}$ are subject of the Newton iteration. We denote by $\mathbf{A}_{jl}$, $j,l \in \{\mathcal{N},\mathcal{S}\}$ the block tangential matrices associated with the basis functions of the free structure nodes ($\mathcal{N}$) and the potential contact nodes ($\mathcal{S}$). The entries of the vectors $\boldsymbol{u}$ and $\boldsymbol{F}$ for $j \in \{\mathcal{N},\mathcal{S}\}$ are denoted by $\boldsymbol{u}_j$ and $\boldsymbol{F}_j$. Let us now discretize the contact conditions. The strong point-wise non-penetration condition (3) is replaced by a weaker integral condition

$$\int_{\Gamma_C} (\boldsymbol{u}\cdot\boldsymbol{n})\, \psi_p \, ds \le \int_{\Gamma_C} g\, \psi_p \, ds, \qquad p \in \mathcal{S}. \tag{11}$$

If we define the right side by g_p and use (10), we can write for the algebraic representation of the weak non-penetration condition

$$u_{n,p} := \boldsymbol{n}_p^\top \mathbf{D}[p,p]\, \boldsymbol{u}_p \le g_p, \qquad p \in \mathcal{S}, \tag{12}$$

where $\boldsymbol{u}_p \in \mathbb{R}^2$ denotes the coefficient vector of $\boldsymbol{u}$ associated with the vertex p and $\boldsymbol{n}_p$ denotes the normal vector at the vertex p. Condition (4) is discretized by $\lambda_{n,p} \ge 0$ at each vertex $p \in \mathcal{S}$, where $\lambda_{n,p}$ is defined according to (12) by $\lambda_{n,p} := \boldsymbol{n}_p^\top \mathbf{D}[p,p]\, \boldsymbol{\lambda}_p$, $\boldsymbol{\lambda}_p \in \mathbb{R}^d$. Introducing the tangential part of the Lagrange multiplier $\boldsymbol{\lambda}$ at the vertex $p \in \mathcal{S}$ by $\boldsymbol{\lambda}_{T,p} := \boldsymbol{\lambda}_p - (\boldsymbol{\lambda}_p\, \boldsymbol{n}_p)\, \boldsymbol{n}_p$ and the vector of internal forces at the node p by $[\boldsymbol{F}(\boldsymbol{u})]_p \in \mathbb{R}^d$, we can rewrite the problems (3) - (6) and (8) in their discrete algebraic form as

$$\begin{aligned} &[\boldsymbol{F}(\boldsymbol{u})]_p + \mathbf{D}[p,p]\boldsymbol{\lambda}_p = 0, \\ &u_{n,p} \le g_p, \ \ \lambda_{n,p} \ge 0, \ \ \lambda_{n,p}(u_{n,p} - g_p) = 0, \\ &\boldsymbol{\lambda}_{T,p} = \mathbf{0} \end{aligned} \tag{13}$$

for all vertices $p \in \mathcal{S}$. We remark, that the conditions in (13) are the Karush–Kuhn–Tucker conditions of a constrained optimization problem for inequality constraints.

Algorithm and equation system Our goal is now to find the correct subset $\mathcal{A}$ of vertices of $\mathcal{S}$, for which the structure is in contact with the tool. To find the correct active set $\mathcal{A}$, we follow an approach given in [12], where this strategy is applied to constrained quadratic optimization problems with inequality constraints. This leads to the primal-dual active set Algorithm 1. Next we give the algebraic representation of line 3–6 in Algorithm 1. To do so, we decompose the diagonal matrix $\mathbf{D}$ into

$$\mathbf{D} = \begin{bmatrix} \mathbf{D}_{\mathcal{I}_k} & \mathbf{0} \\ \mathbf{0} & \mathbf{D}_{\mathcal{A}_k} \end{bmatrix}.$$

Furthermore, we define according to the definition of $u_{n,p}$ in (12) the matrix $\mathbf{N}_{\mathcal{A}_k} \in \mathbb{R}^{|\mathcal{A}_k| \times d|\mathcal{A}_k|}$, where $|\mathcal{A}_k|$ denotes the number of vertices in $\mathcal{A}_k$, by

$$\mathbf{N}_{\mathcal{A}_k} := \begin{bmatrix} \ddots & \mathbf{0}_{1\times d} & \\ \mathbf{0}_{1\times d} & w_{pp}\,\boldsymbol{n}_p & \\ & & \ddots \end{bmatrix}, \qquad p \in \mathcal{A}_k.$$

where w_{pp} is an abbreviation for $\mathbf{D}[p,p]_{1,1} = \cdots = \mathbf{D}[p,p]_{d,d} = \int_{\Gamma_C} \varphi_p \, ds$, having the meaning of a weighting-factor. The associated tangential vectors are then given by $\boldsymbol{t}_p \perp \boldsymbol{n}_p$ in the 2D case and by $\boldsymbol{t}_p^\xi \perp \boldsymbol{n}_p$ and $\boldsymbol{t}_p^\eta := \boldsymbol{t}_p^\xi \times \boldsymbol{n}_p$ with $||\boldsymbol{n}_p|| = ||\boldsymbol{t}_p^\xi|| = ||\boldsymbol{t}_p^\eta|| = 1$ in the 3D case. We define the matrix $\mathbf{T}_{\mathcal{A}_k} \in \mathbb{R}^{|\mathcal{A}_k| \times 2|\mathcal{A}_k|}$, by

$$\mathbf{T}_{\mathcal{A}_k} := \begin{bmatrix} \ddots & \mathbf{0}_{1\times 2} & \\ \mathbf{0}_{1\times 2} & \boldsymbol{t}_p & \\ & & \ddots \end{bmatrix}, \qquad p \in \mathcal{A}_k$$

in the 2D case and

$$\mathbf{T}_{\mathcal{A}_k}^{(m)} = \begin{bmatrix} & \mathbf{0}_{1\times 3} & \\ \mathbf{0}_{1\times 3} & \boldsymbol{t}_p^{(m)} & \\ & & \ddots \end{bmatrix} \in \mathbb{R}^{|\mathcal{A}_k| \times 3|\mathcal{A}_k|}, \quad m = \xi, \eta, \quad p \in \mathcal{A}_k$$

in the 3D case. By $n_{p,i}, \quad i = 1, \ldots, d$, we denote the components of the normal vector. Now the algebraic representation of Algorithm 1, lines 3–6, is given by

$$\begin{bmatrix} \mathbf{A}_{\mathcal{N}\mathcal{N}} & \mathbf{A}_{\mathcal{N}\mathcal{I}} & \mathbf{A}_{\mathcal{N}\mathcal{A}} & \mathbf{0} & \mathbf{0} \\ \mathbf{A}_{\mathcal{I}\mathcal{N}} & \mathbf{A}_{\mathcal{I}\mathcal{I}} & \mathbf{A}_{\mathcal{I}\mathcal{A}} & \mathbf{D}_{\mathcal{I}} & \mathbf{0} \\ \mathbf{A}_{\mathcal{A}\mathcal{N}} & \mathbf{A}_{\mathcal{A}\mathcal{I}} & \mathbf{A}_{\mathcal{A}\mathcal{A}} & \mathbf{0} & \mathbf{D}_{\mathcal{A}} \\ \mathbf{0} & \mathbf{0} & \mathbf{0} & \mathbf{I}_{\mathcal{I}} & \mathbf{0} \\ \mathbf{0} & \mathbf{0} & \mathbf{N}_{\mathcal{A}} & \mathbf{0} & \mathbf{0} \\ \mathbf{0} & \mathbf{0} & \mathbf{0} & \mathbf{0} & \mathbf{T}_{\mathcal{A}} \end{bmatrix} \begin{bmatrix} \boldsymbol{u}_{\mathcal{N}}^i \\ \boldsymbol{u}_{\mathcal{I}}^i \\ \boldsymbol{u}_{\mathcal{A}}^i \\ \boldsymbol{\lambda}_{\mathcal{I}} \\ \boldsymbol{\lambda}_{\mathcal{A}} \end{bmatrix} = \begin{bmatrix} [\mathbf{A}\boldsymbol{u}^{i-1}]_{\mathcal{N}} \\ [\mathbf{A}\boldsymbol{u}^{i-1}]_{\mathcal{I}} \\ [\mathbf{A}\boldsymbol{u}^{i-1}]_{\mathcal{A}} \\ \mathbf{0} \\ \boldsymbol{g}_{\mathcal{A}_k} \\ \mathbf{0} \end{bmatrix} - \begin{bmatrix} \boldsymbol{F}_{\mathcal{N}}(\boldsymbol{u}^{i-1}) \\ \boldsymbol{F}_{\mathcal{I}}(\boldsymbol{u}^{i-1}) \\ \boldsymbol{F}_{\mathcal{A}}(\boldsymbol{u}^{i-1}) \\ \mathbf{0} \\ \mathbf{0} \\ \mathbf{0} \end{bmatrix} \tag{14}$$

with $\mathbf{T}_{\mathcal{A}} = \begin{bmatrix} \mathbf{T}_{\mathcal{A}}^\xi \\ \mathbf{T}_{\mathcal{A}}^\eta \end{bmatrix}$ in the 3D case. Here $\boldsymbol{g}_{\mathcal{A}_k}$ denotes the vector containing the entries g_p associated with the active vertex $p \in \mathcal{A}_k$. The index of the active-set-step k is fixed, and i is the index of the Newton iteration.

3 Iterative solution procedure and implementation

We do not directly solve system (14), because this would mean in the context of a FE-package that the size of the system to be solved always changes if the size of $\mathcal{S}$ is variable from time step to time step. This would be impractical, but due to the dual Lagrange multiplier space, $\boldsymbol{\lambda}$ can be locally eliminated:

$$\boldsymbol{\lambda} = \mathbf{D}^{-1} \left([\mathbf{A}\boldsymbol{u}^{i-1}]_{\mathcal{S}} - [\mathbf{A}\boldsymbol{u}^{i}]_{\mathcal{S}} - \boldsymbol{F}_{\mathcal{S}}(\boldsymbol{u}^{i-1}) \right). \tag{15}$$

To get the reduced system for the displacements $\boldsymbol{u}$, we perform a static condensation of the Lagrange multipliers. The resulting system, written as an incremental Newton scheme, is then:

$$\begin{bmatrix} \mathbf{A}_{\mathcal{N}\mathcal{N}} & \mathbf{A}_{\mathcal{N}\mathcal{I}} & \mathbf{A}_{\mathcal{N}\mathcal{A}} \\ \mathbf{A}_{\mathcal{I}\mathcal{N}} & \mathbf{A}_{\mathcal{I}\mathcal{I}} & \mathbf{A}_{\mathcal{I}\mathcal{A}} \\ \mathbf{0} & \mathbf{0} & \mathbf{N}_{\mathcal{A}} \\ \mathbf{T}_{\mathcal{A}}\mathbf{A}_{\mathcal{A}\mathcal{N}} & \mathbf{T}_{\mathcal{A}}\mathbf{A}_{\mathcal{A}\mathcal{I}} & \mathbf{T}_{\mathcal{A}}\mathbf{A}_{\mathcal{A}\mathcal{A}} \end{bmatrix} \begin{bmatrix} \Delta\boldsymbol{u}^i_{\mathcal{N}} \\ \Delta\boldsymbol{u}^i_{\mathcal{I}} \\ \Delta\boldsymbol{u}^i_{\mathcal{A}} \end{bmatrix} = - \begin{bmatrix} \boldsymbol{F}_{\mathcal{N}}(\boldsymbol{u}^{i-1}) \\ \boldsymbol{F}_{\mathcal{I}}(\boldsymbol{u}^{i-1}) \\ -\boldsymbol{g}_{\mathcal{A}} + \mathbf{N}_{\mathcal{A}}\boldsymbol{u}^{i-1}_{\mathcal{A}} \\ \mathbf{T}_{\mathcal{A}}\boldsymbol{F}_{\mathcal{A}}(\boldsymbol{u}^{i-1}) \end{bmatrix} \tag{16}$$

with $\Delta\boldsymbol{u} := \boldsymbol{u}^i - \boldsymbol{u}^{i-1}$. This system must be solved in every Newton step. The computational effort of calculating $\boldsymbol{\lambda}$ in (15) can be reduced by applying:

$$\boldsymbol{\lambda} \approx -\mathbf{D}^{-1}\boldsymbol{F}_{\mathcal{S}}(\boldsymbol{u}^{i-1}) \tag{17}$$

because during the Newton iteration $||[\mathbf{A}\boldsymbol{u}^{i-1}]_{\mathcal{S}} - [\mathbf{A}\boldsymbol{u}^i]_{\mathcal{S}}||$ is small in comparison to $||\boldsymbol{F}_{\mathcal{S}}(\boldsymbol{u}^{i-1})||$ because $\boldsymbol{F}_{\mathcal{S}}$ contains the internal forces which balance the contact forces. Or in other words: At the end of the Newton iteration $\boldsymbol{\lambda}$ is the projection of the contact forces onto $\text{span}\{\psi_q\}^d$.

3.1 Active Set Strategy and Algebraic Multigrid Methods

Algorithm 2 Exact strategy

1: make a choice for $\mathcal{A}_1$ and $\mathcal{I}_1$
2: **for** $k = 1, \ldots$ **until** $\mathcal{A}_{k+1} = \mathcal{A}_k$ **do**
3: **for** $i = 1, \ldots$ **until** Newton convergence **do**
4: **assemble** tangential stiffness $\mathbf{A}^{k,i}$ and force–vector $\boldsymbol{F}(\boldsymbol{u}^{k,i-1})$
5: **introduce** the contact conditions into the system $\mathbf{A}^{k,i}\Delta\boldsymbol{u}^{k,i} = -\boldsymbol{F}(\boldsymbol{u}^{k,i-1})$ according to (16)
6: **solve** the resulting system with the iterative solver:
7: **for** $l = 1, \ldots,$ until AMG convergence **do**
8: $\Delta\boldsymbol{u}^{k,i,l} := AMG(\Delta\boldsymbol{u}^{k,i,l-1}, \mathbf{A}^{k,i}, \boldsymbol{F}(\boldsymbol{u}^{k,i-1}))$
9: **end for**
10: $\Delta\boldsymbol{u}^{k,i} := \Delta\boldsymbol{u}^{k,i,l}$
11: $\boldsymbol{u}^{k,i} := \boldsymbol{u}^{k,i-1}\Delta\boldsymbol{u}^{k,i}$
12: **end for**
13: **calculate** $\boldsymbol{\lambda}^k$ according to (17)
14: **update** $\mathcal{A}_{k+1}$ and $\mathcal{I}_{k+1}$ according to Algorithm $1_{\text{line 8,9}}$
15: **end for**

Our aim is now to solve the linearized equation system (16). Multigrid methods have proven to be highly efficient for problems arising from finite element discretizations of partial differential equations, see e.g. [7]. Due to the fact that locally refined meshes are widely used throughout engineering practice for such kind of problems a hierarchical grid structure might be very difficult to achieve on large unstructured grids. For that reason we concentrate on algebraic multigrid methods as they preserve the main multigrid properties but require only the system matrix and thus appear to be very attractive. Algebraic multigrid (AMG), which was first introduced by Brandt, McCormick, Ruge and Stüben in the 1980's has received steady progress in its development since, to become a robust and efficient tool in numerics, see e.g. [6] and the references therein, as well as it has been applied to a wide field of applications, including structural mechanics. Although the initial attempts were restricted to M-matrices, it has been shown that the method works well also for other matrices in many cases. For the according theory we refer to [5, 18, 19]. A vital property of a method to be used in engineering is a generalized applicability to different problems and therefore the reduction of parameters to be chosen before use. Thus, a compromise has to be found to fulfill that demand and still maintain maximum performance. In order to do so, in this study we use the classical Ruge-Stüben AMG method in a scalar approach to preserve the property of a total black-box solver and ensure a generalized applicability as issued.

For further acceleration the AMG will be used as a preconditioner for a conjugate gradient method, which has proven to be very efficient [19, 4]. Due to the fact that the emerging equation systems are slightly unsymmetric matrices when used in connection with the active set strategy a BiCGStab method is used when necessary. Each AMG-cycle consists of two full Gauß-Seidel iterations for pre- and post-smoothing on each level of a standard V-cycle and a direct sparse Gauß-elimination on the coarsest level. It has to be observed that in case of the BiCGStab method two AMG cycles are performed per iteration due to the symmetry of the method. For simplicity we will denote the according AMG-preconditioned CG method by AMG method in the rest of the paper. In the following, it will be examined how those methods perform in combination with the described active set strategy, and the developed algorithms are discussed.

3.2 Inexact strategies

Algorithm 3 Newton-inexact strategy

1: make a choice for $\mathcal{A}_1$ and $\mathcal{I}_1$
2: **for** $i = 1, \ldots$ **until** Newton convergence and $\mathcal{A}_i = \mathcal{A}_{i-1}$ **do**
3: **assemble** tangential stiffness $\mathbf{A}^i$ and force-vector $\boldsymbol{F}(u^{i-1})$
4: **introduce** the contact conditions into the system $\mathbf{A}^i \Delta \boldsymbol{u}^i = -\boldsymbol{F}(\boldsymbol{u}^{i-1})$ according to (16)
5: **solve** the resulting system with the iterative solver:
6: **for** $l = 1, \ldots,$ until AMG-convergence **do**
7: $\Delta \boldsymbol{u}^{i,l} := AMG(\Delta \boldsymbol{u}^{i,l-1}, \mathbf{A}^i, \boldsymbol{F}(u^{i-1}))$
8: **end for**
9: $\Delta \boldsymbol{u}^i := \Delta \boldsymbol{u}^{i,l}$
10: $\boldsymbol{u}^i := \boldsymbol{u}^{i-1} \Delta \boldsymbol{u}^i$
11: **calculate** $\boldsymbol{\lambda}$ according to (17)
12: **update** $\mathcal{A}_{i+1}$ and $\mathcal{I}_{i+1}$ according to Algorithm $1_{\text{line 8,9}}$
13: **end for**

Two strategies are possible to organize the Newton loop and the active set loop: The so called exact strategy where the loops are nested and two inexact strategies with unrolled loops, described in the following. First we consider the complete exact Algorithm 2. By $\boldsymbol{u}^{k,i,l}$ we denote the solution in the active set step k, the Newton iteration i and the AMG iteration l. In the Newton-inexact strategy Algorithm 3 the active-inactive-decision in Algorithm $1_{\text{line 8,9}}$ is done within each Newton step. That means that in the inexact strategy the two nonlinearities of material behavior and contact can be handled in only one Newton loop. This is possible, because the search for the correct active set can also be interpreted as a Newton iteration [12].

In the inexact case the constant $c > 0$ in Algorithm $1_{\text{line 8,9}}$ has the meaning of a weighting between the non-penetration condition (3) and the contact stress condition (4) in the inactive-active-decision. In the exact case, the c doesn't play any role because pressure ($\lambda > 0$) without penetration ($\boldsymbol{u} \cdot \boldsymbol{n} - g < 0$) cannot occur. Also the case tension ($\lambda < 0$) and penetration ($\boldsymbol{u} \cdot \boldsymbol{n} - g > 0$) does not exist either. The next step to improve the performance even further is to combine Algorithm 3 with the iterative solving process. The strategy to reduce the total number of AMG cycles per time step is to perform only a few AMG steps (m small) in the first Newton iterations because in these it is not efficient to iterate the AMG until convergence since the first iterates will be very far from the solution anyway. We call this strategy AMG-inexact strategy and write it down in the Algorithm 4.

4 Numerical results

In this section, we will give some numerical results to show the performance of the suggested algorithms. For that reason, on the one hand the active set strategy is compared to a standard contact formulation namely the penalty formulation, which is widely used throughout engineering

Algorithm 4 AMG-inexact strategy

1: make a choice for $\mathcal{A}_1$ and $\mathcal{I}_1$
2: **for** $i = 1, \ldots$ **until** Newton convergence and $\mathcal{A}_i = \mathcal{A}_{i-1}$ **do**
3: **assemble** tangential stiffness $\mathbf{A}^i$ and force-vector $\boldsymbol{F}(\boldsymbol{u}^{i-1})$
4: **introduce** the contact conditions into the system $\mathbf{A}^i \Delta \boldsymbol{u}^i = -\boldsymbol{F}(\boldsymbol{u}^{i-1})$ according to (16)
5: **for** $l = 1, \ldots, m$ **do**
6: $\Delta \boldsymbol{u}^{i,l} := AMG(\Delta \boldsymbol{u}^{i,l-1}, \mathbf{A}^i, \boldsymbol{F}(\boldsymbol{u}^{i-1}))$
7: **end for**
8: $\Delta \boldsymbol{u}^i := \Delta \boldsymbol{u}^{i,l}$
9: $\boldsymbol{u}^i := \boldsymbol{u}^{i-1} \Delta \boldsymbol{u}^i$
10: **calculate** $\boldsymbol{\lambda}$ according to (17)
11: **update** $\mathcal{A}_{k+1}$ and $\mathcal{I}_{k+1}$ according to Algorithm $1_{\text{line 8,9}}$
12: **end for**

practice. On the other hand a comparison is shown between the algebraic multigrid solver and other classical iterative schemes. Finally further examples are given by using the two inexact strategies we suggested above and an elasto-plastic constitutive law respectively.

4.1 Test case

In the following, we consider the example depicted in Figure 3, where we indent a block of dimension $100 \times 100 \times 50$ by a hemispherical rigid punch with radius 30 by the depth $d = 5$ within one time step. If not stated else the block is discretized by linear hexahedral elements and an underlying constitutive law of nonlinear elasticity. For further information we refer to [1, 8].

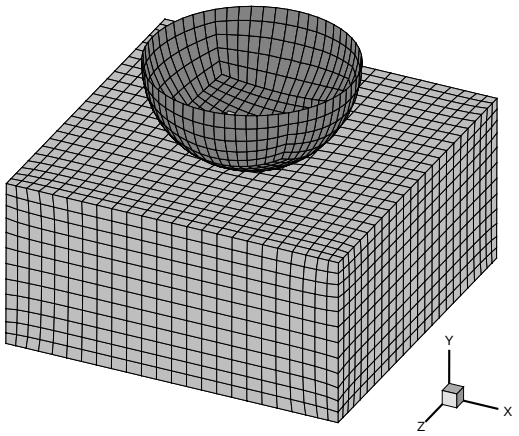

Figure 3: Setting of the contact problem

4.2 Comparison of both contact approaches in connection with AMG

The penalty method can be formulated for the potential contact nodes $p \in \mathcal{S}$:

$$[\boldsymbol{F}(\boldsymbol{u})]_p^\top \cdot \boldsymbol{n}_p + \rho(\boldsymbol{u}_p \cdot \boldsymbol{n}_p - g_p)_+ = 0, \quad p \in \mathcal{S},$$

where $(x)_+ := \frac{1}{2}(|x| + x)$. So the penetration in the normal direction is penalized by the artificial spring force with the spring rate ρ. This constant must be of significant size ($10^8 - 10^{10}$ are common values) to avoid penetration of the bodies and ensure high accuracy. Figure 4 resp. Table 1 illustrate the mentioned behavior.

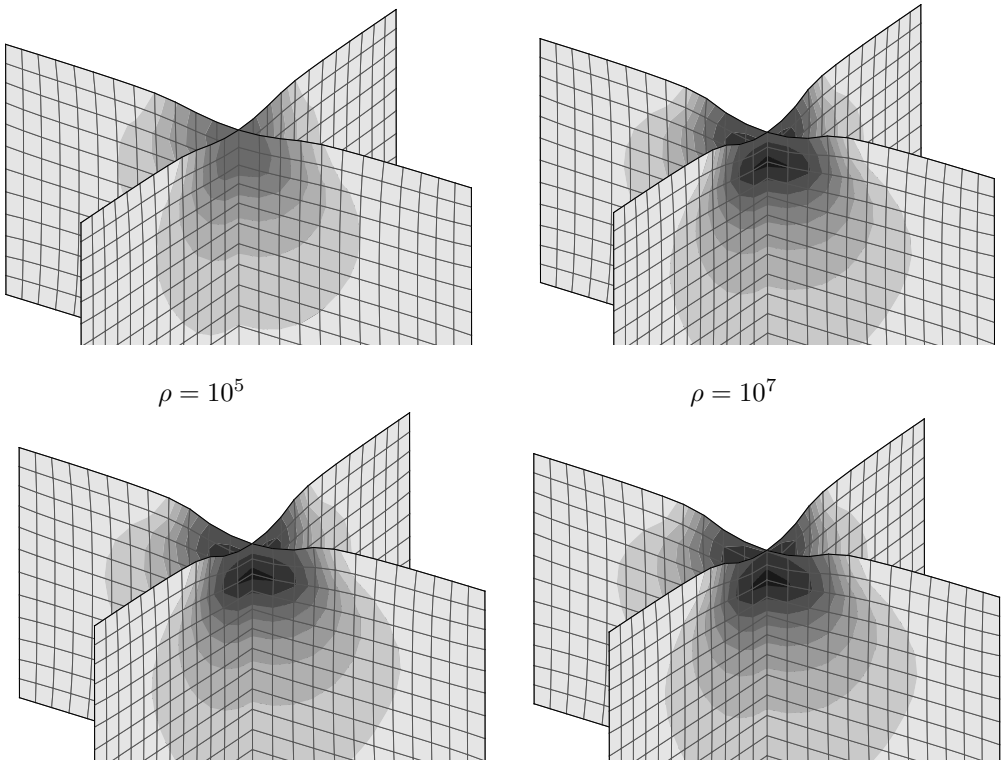

Figure 4: Deformed shape, loss in accuracy with decreasing penalty factor and active set strategy, von Mises equivalent stress σ_{seqv}

Unfortunately the need for a large penalty value ρ is contradictory to the requisites of iterative solvers since the penalty factor deteriorates the condition numbers of the emerging equation systems, and thus entails iterative solvers to struggle bad convergence rates. This problem can be significantly improved by using the primal dual active set strategy as illustrated below. Figure 5 shows the convergence histories for the solution of the arising equation system in a representative Newton step, on the one hand using a penalty formulation ($\rho = 10^9$) and on the other hand the active set strategy (ASeS). In both cases the algebraic multigrid solver is applied.

4.3 Active set versus adaptive penalty strategies

We compare in Figure $6_{\mathbf{A}}$ the average computation time per Newton step for the active set strategy (a) and the following different penalty strategies p1-p5 with the penalty parameter $\rho = 10^{i_k}$ in

Table 1: Comparison of results with decreasing penalty factor and active set strategy (ASeS)

method	displacement $d_{y,min}$	Mises equiv. stress $S_{eqv,max}$
$\rho = 10^5$	-2.79	5665
$\rho = 10^7$	-4.86	8370
$\rho = 10^9$	-4.89	8399
ASeS	-4.99	8398

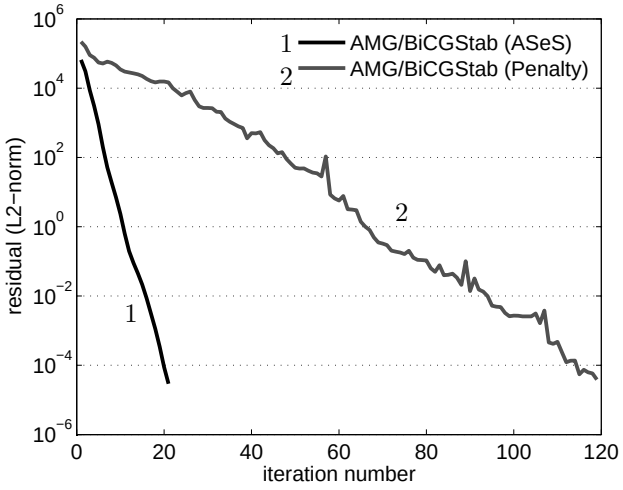

Figure 5: Residual reduction per iteration. ASeS resp. penalty approach and AMG-solver

the kth Newton step.

$$\begin{aligned} p1: &\quad i = 2,4,6,8,9 \\ p2: &\quad i = 4,9 \\ p3: &\quad i = 6,8,9 \\ p4: &\quad i = 4,7,9 \\ p5: &\quad i = 9 \\ a: &\quad - \end{aligned}$$

Here for example $i = 6,8,9$ means: The penalty parameter ρ is 10^6 in the first, 10^8 in the second and 10^9 in all the Newton steps during the rest of the time step. One sees that the computation time for the active set is significantly smaller in comparison to, e.g. penalty strategy p5, where a high penalty value is chosen right from the start. The explanation is that the contact penalty deteriorates the condition of the stiffness matrix as mentioned before and therefore slows down the convergence of the iterative solver [7, 5]. But one could think that there are clever strategies which work adaptively in that sense that they start with a small penalty value in the first Newton steps and choose the expensive high penalty value only in the last Newton steps like it is done in the strategies p1-p4. Figure $6_{\mathbf{B}}$ shows that this does not work out because low penalty values in the beginning compel us to take more Newton steps, since we have a large penetration in the beginning and we therefore undermine the convergence of the Newton method. Only the strategy p3 performs quite well but for this strategy as well as for the others we need much more total computation time over the whole time step than the active set strategy, see Figure $6_{\mathbf{C}}$. We can conclude that the convergence speed of iterative solvers is significantly lower when using a penalty formulation, no matter if we use a high value right from the start or if we use an adaptive strategy.

4.4 Performance of different solvers using the active set strategy

To show the behavior of different solvers using the active set strategy, we use different discretizations of the block and recalculate the given example with a direct solver, classical Gauß-Seidel iterations, a Conjugate Gradient method with Gauß-Seidel preconditioning (GS-CG) and finally the described algebraic multigrid method (AMG-CG). Figure 7 (left) shows the computation time per Newton step averaged over the time step. We get the well known result that iterative solvers perform much better than the direct solver applied on fairly well conditioned problems of moderate

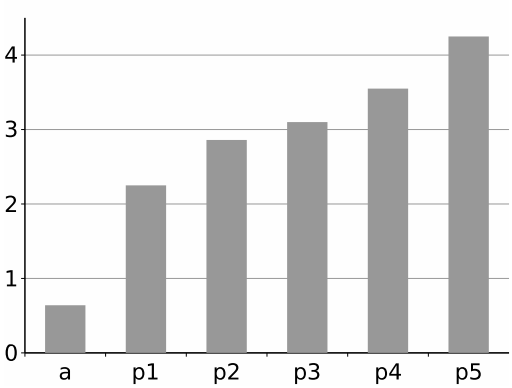

(A) Averaged computation time per Newton step in seconds

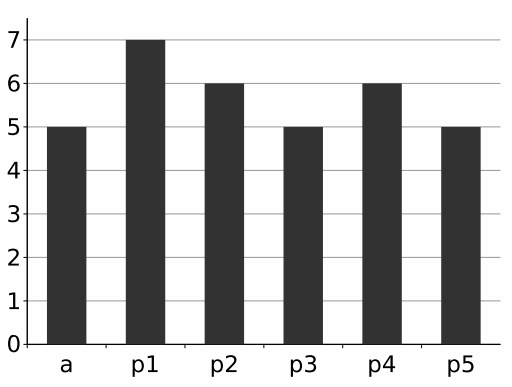

(B) No. of Newton steps

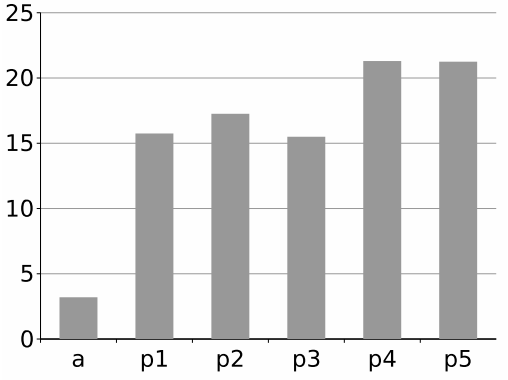

(C) Total computation time per time step in seconds

Figure 6: Comparison between active set strategy (a) and different adaptive penalty strategies (p1-p5)

size. The right part of Figure 7 is the same picture with higher resolution for the iterative solvers. Here we see that the described AMG performs best among these solvers already at a moderate number of degrees of freedom and also exhibits best complexity.

4.5 Further acceleration by AMG-inexact strategy

As mentioned above further acceleration can be achieved by an inexact strategy according to Algorithm 4 in Section 3.2. Figure 8 resp. Table 2 describe the parameter settings and show the numerical results for the issued simulations.
In the strategy i4 for example (see Figure 8, Table 2), the number of AMG cycles m is fixed to $1, 1, 2$ in the first three Newton-Raphson steps (NR steps) and during the rest of the time step we let the solver iterate until convergence. In contrast the exact strategy i1, in which we always await AMG convergence, has altogether much more solver cycles and therefore a larger computation time. Other 'semi-inexact' examples with a variable number of solver cycles are given in the strategies i2 and i3. It is even possible to perform the totally inexact strategy given in i5, where we perform only one AMG cycle per Newton step, which means that Newton loop and solver loop coincide now. Although the total number of AMG cycles is 15 as in case i4, this totally inexact

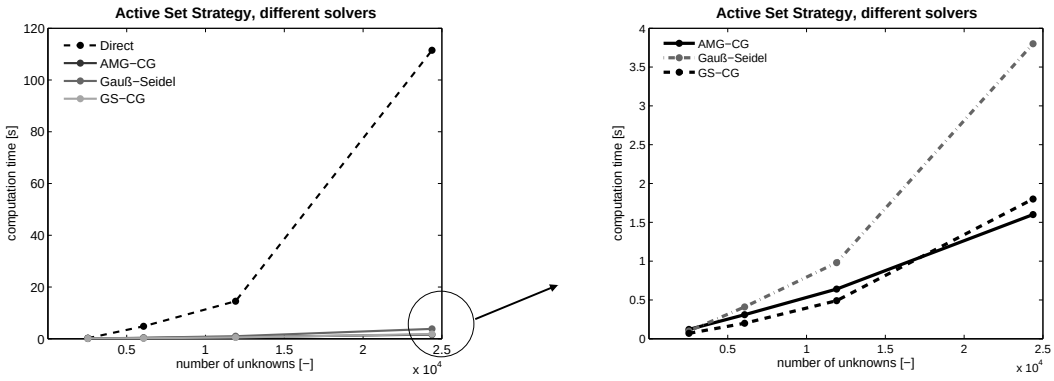

Figure 7: Averaged computation time per Newton step of direct and iterative solvers in connection with active set strategy

strategy needs more computation time than the semi-inexact one. This can be explained by the fact, that in strategy i5 the setup of the AMG solver must be initialized more often, since we perform more Newton steps and thus, we have more different equation systems. This again could be overcome by preserving the coarse grid levels from one Newton step to another but it has to be observed that the active set might change and has to be correctly represented on the coarse grids. By applying the whole setup phase in each Newton step this problem is avoided. Using an adaptive strategy would be appealing but then again the black-box character of the described method is lost to some extent.

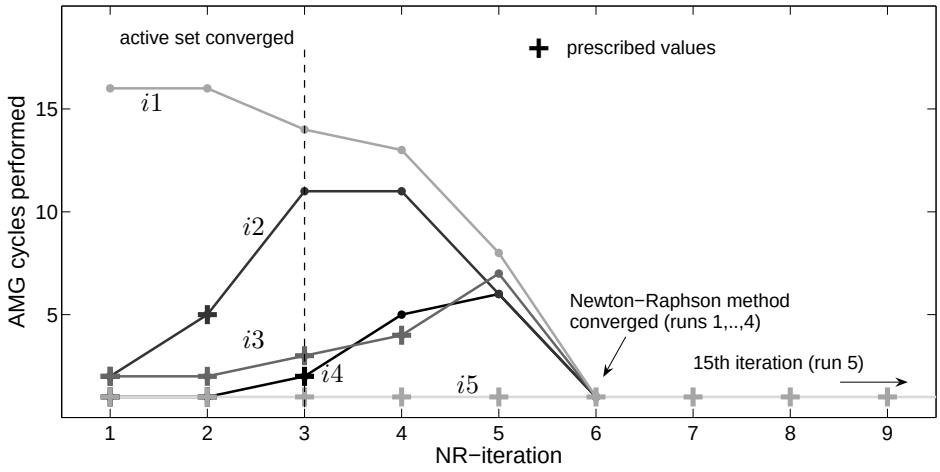

Figure 8: Active set strategy and AMG with loop unrolling

4.6 Test case and elasto-plastic material model

In the last example, we demonstrate that apart from elasticity, it is also possible to compute models including other constitutive laws. In the given case an elasto-plastic material law is used. The elastic part can be described by Hooke's law whereas for the plastic part an appropriate yield function and equations for the description of the plastic flow are provided. For further theory and implementation details we refer to [1, 8]. For theoretical results in plasticity we refer to the textbook [9] and for theoretical results in contact and plasticity we refer to [10, 11, 17]. The block given in the test case is indented by the hemispherical sphere by the depth of $d_y = -1$ in each of 10 time steps. The active set strategy as well as the AMG solver are the applied solution methods.

Table 2: Inexact strategy, convergence history of respective loops

run	NR steps with prescribed values (m_i)	NR step of active set convergence	NR step with NR loop convergence	total AMG cycles	total time [s]
i1	-	3	6	67	10.2
i2	2 (2,5)	3	6	35	8.1
i3	4 (2,2,3,4)	3	6	18	5.7
i4	3 (1,1,2)	3	6	15	5.1
i5	all (1,1,...)	3	15	15	8.9

Figure 9 depicts the results obtained for the three time steps t_2, t_5 and t_{10}. The total equivalent plastic strain (ETAQ) is shown. Three quarters of the model are blanked only for reasons of illustration. The results endorse the observations that the described method is very robust and as well features applicability beyond the case of elasticity.

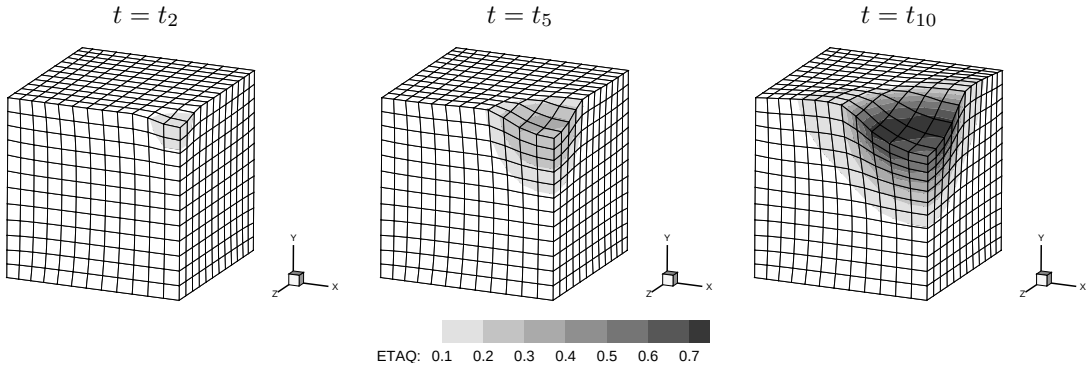

Figure 9: Active set strategy and AMG, elasto-plastic material law

5 Summary

In this paper, we presented a method which allows to apply fast iterative solvers on non-linear problems in a very efficient way. It was shown, that the discussed algebraic multigrid methods gain significantly in efficiency in comparison to standard penalty approaches when used in combination with a primal-dual active set strategy and applied on structural mechanics contact problems. Furthermore it was shown that computation time can be further decreased by merging the otherwise nested loops of each method into a single solver loop by the described inexact strategies. The theory explained exhibits the character of the method and a way to implement the method in a practical manner into a FE-package. The study is based on a very simple approach for the algebraic multigrid in order to preserve the black-box applicability of the method to a maximum extent.

6 Ackknowledgements

The work in this paper was funded by the German Research Foundation (DFG) through the projects SCHA814/10-1 and WO671/4-1 in the framework of SPP1146: Modeling of incremental forming operations.

References

[1] T. Belytschko and W.K. Liu and B. Moran, *Nonlinear Finite Elements for Continua and Structures*, John Wiley & Sons, 2000

[2] F. Ben Belgacem, P. Hild, and P. Laborde, *Extension of the mortar finite element method to a variational inequality modeling unilateral contact*, Math. Models Methods Appl. Sci., 9 (1999), pp. 287–303

[3] F. Ben Belgacem and Y. Renard, *Hybrid finite element methods for the Signorini problem*, Mathematics of Computating, 72(243):1117-1145, 2003

[4] M. Benzi, *Preconditioning techniques for large linear systems: a survey*, Journal of Computational Physics 182, pp. 418-477, 2002

[5] W.L. Briggs and V.E. Henson and S. McCormick, *A Multigrid Tutorial*, 2nd Edition, SIAM, Philadelphia, 2000

[6] A.J. Cleary and R.D. Falgout and V.E. Henson and J.E. Jones and T.A. Manteuffel and S.F. McCormick and G.N. Miranda and J.W. Ruge, *Robustness and scalability of algebraic multigrid*, SIAM, J. Sci. Comp., Vol.21, No. 5, pp. 1886-1908, Philadelphia, 2000

[7] W. Hackbusch, *Multi-Grid Methods and Applications*, Springer, Berlin Heidelberg New York Tokyo, 1985

[8] R. Diez, U. Hindenlang and A. Kurz, *LARSTRAN User's manual – LARSTRAN documentation*, Stuttgart, 1996

[9] W. Han and B.D. Reddy, *Plasticity, Mathematical Theory and Numerical Analysis*, Springer, 1999

[10] W. Han and M. Sofonea, *Numerical analysis of a frictionless contact problem for elastic- viscoplastic materials*, Comput. Methods Appl. Mech. Engrg., 190(1-2):179–191, 2000

[11] W. Han and M. Sofonea, *Quasistatic contact problems in viscoelasticity and viscoplasticity*, American Mathematical Society, International Press, 2002

[12] M. Hintermüller, K. Ito and K. Kunisch, *The primal-dual active set strategy as semi-smooth Newton method*, SIAM J. Optim., 13(3):865–888, 2003

[13] S. Hüeber and B. Wohlmuth, *A primal–dual active set strategy for non–linear multibody contact problems*, Computer Methods in Applied Mechanics and Engineering, 194 (2005), pp. 3147–3166

[14] N. Kikuchi and Y. Song, *Penalty/finite-element approximation of a class of unilateral problems in linear elasticity*, Quarterly of Applied Mathematics, 39(1):1-22, 1981

[15] T.A. Laursen, *Computational Contact and Impact Mechanics*, Springer, 2002

[16] M.A. Puso and T.A. Laursen, *A mortar segment-to-segment contact method for large deformation solid mechanics*, Computat. Methods Appl. Mech. Engrg. 193 (2004) pp. 601-629

[17] M. Rochdi and M. Sofonea, *On frictionless contact between two elastic- viscoplastic bodies*, Quart. J. Mech. Appl. math., 50(3):481–496, 1997

[18] J.W. Ruge and K. Stüben, *Algebraic Multigrid*, Multigrid Methods, Frontiers in Applied Mathematics, S. McCormick, SIAM, Philadelphia, 1987

[19] K. Stüben, *Algebraic Multigrid (AMG), An introduction with applications*, GMD Report 70, St. Augustin, 1999

[20] B. Wohlmuth, *A mortar finite element method using dual spaces for the Lagrange multiplier*, SIAM J. Numer. Anal., 38 (2000), pp. 989–1012

[21] P. Wriggers and K. Fischer, *Recent new developments in contact mechanics*, Proceedings of the 4$^{\text{th}}$ European LS-DYNA Users Conference, Ulm, 2003

[22] P. Wriggers and K. Fischer, *Frictionless 2D contact formulations for finite deformations based on the mortar method*, Computational Mechanics (2005) 36: 226-244

[23] P. Wriggers,*Computational Contact Mechanics*, John Wiley & Sons, 2002

[24] P. Wriggers and G. Zavarise, *Computational Contact Mechanics*, Encyclopedia of Computational Mechanics, Volume 2: Solids and Structures, John Wiley and Sons, 2004

Erschienene Preprints ab Nummer 2005/001

Komplette Liste: `http://preprints.ians.uni-stuttgart.de`

2005/001 *S. Nicaise, A.-M. Sändig:* Dynamical crack propagation in a 2D elastic body. The out-of plane state.

2005/002 *S. Hüeber, A. Matei, B.I. Wohlmuth:* A mixed variational formulation and an optimal a priori error estimate for a frictional contact problem in elasto-piezoelectricity

2005/003 *A.-M. Sändig:* Distributionentheorie mit Anwendungen auf partielle Differentialgleichungen. Vorlesung im Wintersemester 2004/2005

2005/004 *A.-M. Sändig, T. Buchukuri, O. Chkadua, D. Natroshvili:* Solvability and regularity results to boundary-transmission problems for metallic and piezoelectric elastic materials

2005/005 *B. Flemisch, B. I. Wohlmuth:* Stable Lagrange multipliers for quadrilateral meshes of curved interfaces in 3D

2005/006 *Geis, W.:* Determination of stress singularities in piezoelectric stack actuators

2005/007 *Geis, W.:* Numerical simulation of linear models for piezoelectric stack actuators

2005/008 *Sändig, A.-M.:* Mathematische Methoden in der Kontinuumsmechanik. Vorlesung im Sommersemester 2005

2005/009 *Lehrstuhl N.N. (Wendland), Lehrstuhl Wohlmuth, Abteilung Sändig, Abteilung Gekeler:* Jahresbericht 2005

2005/010 *Brunßen, S., Schmid, F., Schäfer, M., Wohlmuth, B.:* A fast and robust method for contact problems by combining a primal-dual active set strategy and algebraic multigrid methods